

Cyclisation of Alkoxy Radicals. A Semiempirical MNDO-PM3 Study

Ivan O. Juranić,* Mihailo Lj. Mihailović and Milan M. Dabović

Faculty of Chemistry, P.O.B. 550, 11001 Belgrade and Institute of Chemistry, Technology and Metallurgy, Njegoševa 12, Belgrade, Yugoslavia

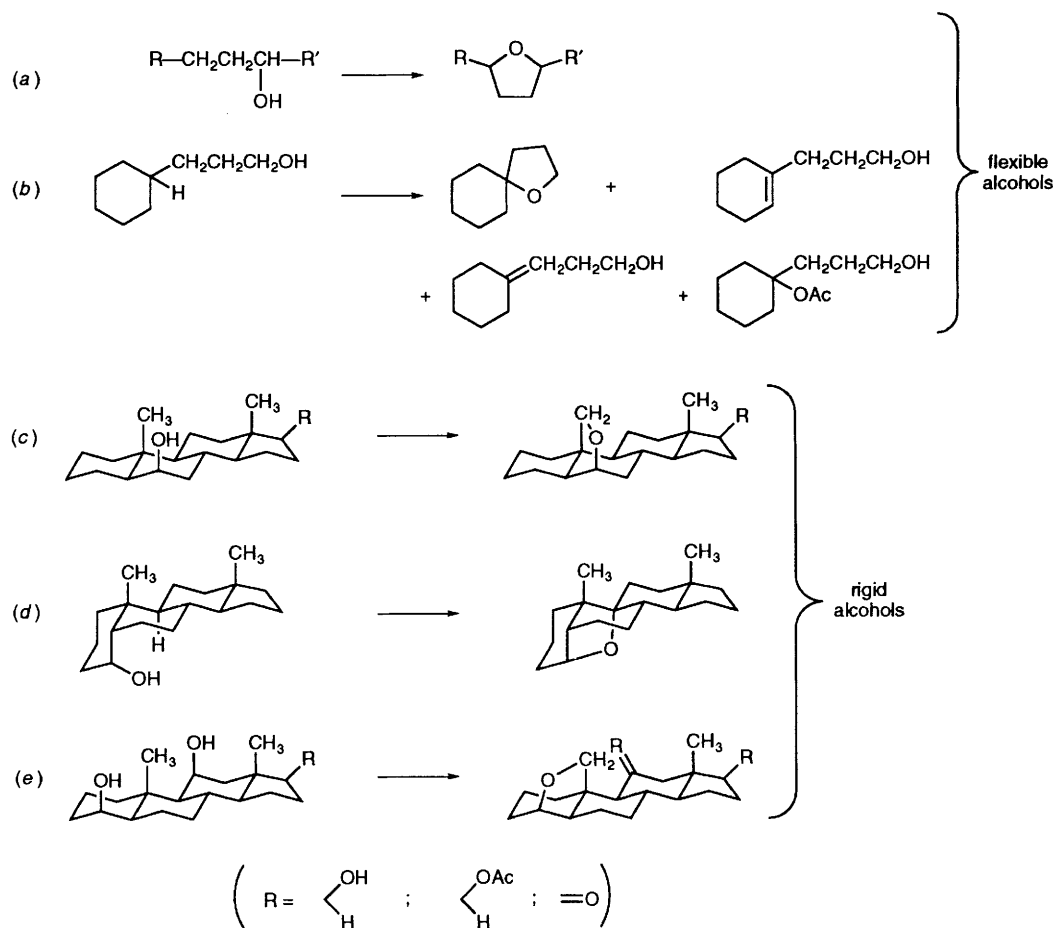
The reactivity of the butoxy and 3-methylcyclohexyl radicals, as representatives of alkoxy radicals, was studied by MNDO-PM3 semiempirical MO method. In both cases it was found that the oxy radical underwent easily 1,5-H migration giving a δ -hydroxyalkyl radical. The hydrogen abstraction reaction goes through two transition states. The first transition state (TS) with short O–H distance has an energy very similar to, or lower than, the TS for 1,5-H migration. The second TS is of higher energy and is much product-like. The overall cyclisation reaction has a high activation energy (over 40 kcal mol⁻¹), and is therefore unlikely to occur spontaneously. Most likely, the cyclisation step needs assistance of some other surrounding molecules to speed up the reaction.

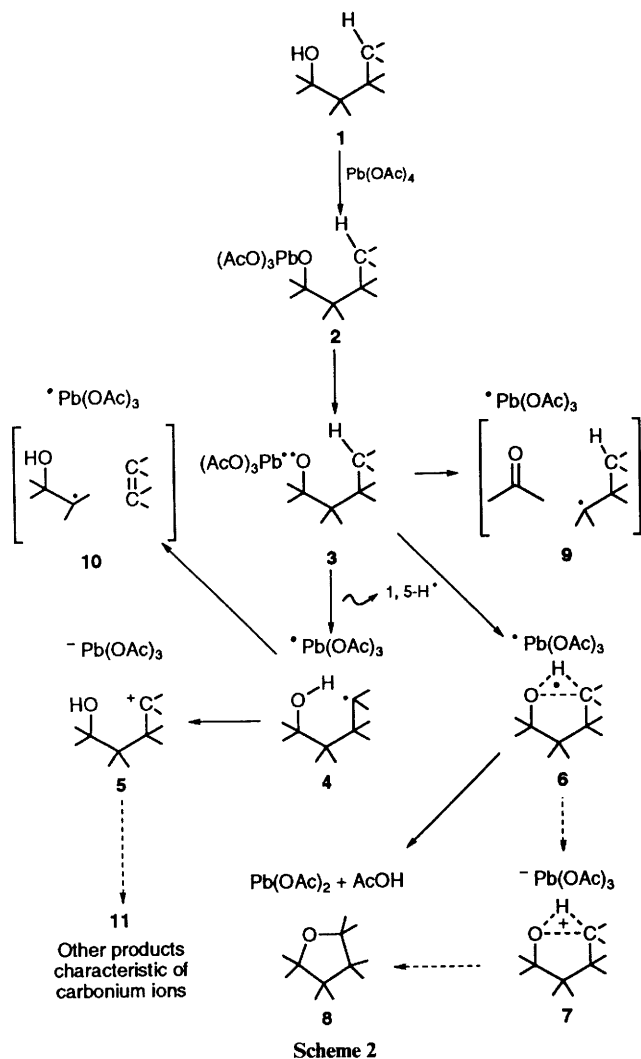
The reaction of alcohols with lead tetraacetate [Pb(OAc)₄] in non-polar solvents (usually benzene), performed thermally (at 80 °C) or UV-photochemically (at 20 °C), affords in general, as shown in Scheme 1, tetrahydrofuran-type ethers as major products.¹

The possible mechanistic pathways for these reactions are shown on Scheme 2. In the case of *conformationally mobile alcohols* [examples (a) and (b) in Scheme 1], i.e. alcohols in which one or both reacting centres [C–OH and/or C(δ)–H], because of free rotation, are flexible, the cyclisation process may be accompanied by other reactions, such as homolytic fragmentation (3→9, 4→10, Scheme 2), and/or heterolytic formation of by-products 11 (olefinic alcohols, acetoxy com-

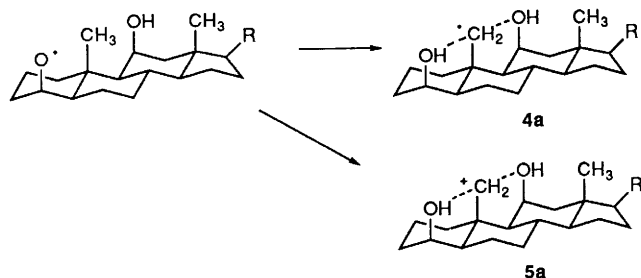
pounds, rearranged products) derived from the δ -carbonium ion-type intermediate 5.

In the case of *conformationally rigid alcohols* [i.e. alcohols in which both reacting centres C–OH and C(δ)–H are rigidly fixed], having an optimal distance (~ 0.25 nm) between the hydroxylic oxygen and the δ -carbon atom (to be functionalised), a convenient spatial orientation of the hydroxylic oxygen and the C(δ)–H bond (to be attacked) and no serious steric interactions preventing approach of Pb(OAc)₄ [examples (c)–(e) in Scheme 1], the cyclisation reaction to ethers of type 8 is usually not accompanied by the formation of secondary products derived from intermediates of type 3, 4 and 5 (even when the β -carbon and δ -carbon atoms are tertiary).





It should be noted that when using a similar substrate (*i.e.* a rigidly fixed alcohol) containing a second, with respect to the δ -carbon atom symmetrically oriented, equidistant and likewise fixed hydroxy group [such as in example (e) in Scheme 1], only one of the ether products of type **8** was detected. It seems that no 'symmetrical intermediates' or transition states of type **4a** and **5a** (Scheme 3) are involved in this reaction.



The question about the extent and kind of interactions between C(δ), H and O in **3** and **4** (Scheme 2) is of importance, since the correct answer could be the key for the rationalisation of the experimental results presented above.

Calculations

In order to elucidate the mechanism of this reaction, we have undertaken a theoretical study of closely related reactions by

Table 1 Energies of different structures of the radical species derived from butan-1-ol and *cis*-3-methylcyclohexanol

Structure	$\Delta H_f/\text{kcal mol}^{-1}$	
	C ₄ H ₉ O	C ₇ H ₁₃ O
C-radical, extended or diequatorial	-30.76	-41.65
C-radical, gauche or diaxial	-33.41	-41.59
O-radical, extended or diequatorial	-23.23	-29.52
O-radical, gauche or diaxial	-21.85	-27.09
Cyclic ether + H (<i>ca.</i> 0.4 nm apart)	-4.31	-4.52
TS for 1,5-H migration	-0.076	-6.65
TS for 1,4-OH migration	-1.392	-4.62
TS for hydrogen abstraction	10.692	9.131

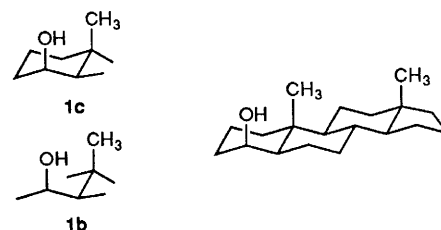


Fig. 1 Starting geometry of the model compound *cis*-3-methylcyclohexanol (**1c**) and of butan-1-ol (**1b**), most resembling the steroid conformation

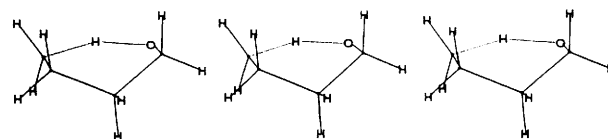


Fig. 2 Stereoview representation (conforming convention in ref. 7) of the transition state, **6b-1**, for 1,5-H migration in the butoxy radical, calculated by the MNDO-PM3 method

use of the semiempirical MNDO PM3 scheme. The MNDO procedure has proven to be fairly reliable for studying molecular properties of heteronuclear radicals in many previous studies.² We used the MOPAC program package, Version 6.01. Odd-electron systems were calculated by 'half-electron' method. The optimised geometries of all molecules were obtained by the force field minima in vacuum according to the PM3 method. The program was installed on IBM 3090 and IBM AT 386 computers.

As a model compound, *cis*-3-methylcyclohexanol, **1c**, *i.e.* the corresponding *cis*-3-methylcyclohexyloxy radical, **3c** (see Scheme 2), was selected. In order to mimic the steric relationships in conformationally rigid alcohols, some of the calculations were performed starting from the diaxial conformation of the model compound, as shown in Fig. 1.

To prove the reliability of the method applied, the calculations on the butoxy radical were performed, too. This radical was already thoroughly investigated by different theoretical methods,³ providing a suitable reference system.

Results and Discussion

Notation of molecules and intermediates is as follows: the bold numerals relate to the assignments given in Scheme 2. Suffix **b** stands for compounds and intermediates derived from butan-1-ol; and suffix **c** stands for compounds and intermediates derived from *cis*-3-methylcyclohexanol in its diaxial conformation. The hydrogen atom subjected to the migration/abstraction is marked as H(μ).

1,5-H Migration.—This type of hydrogen migration has already been studied in alkyl radicals.⁴ It was found that the

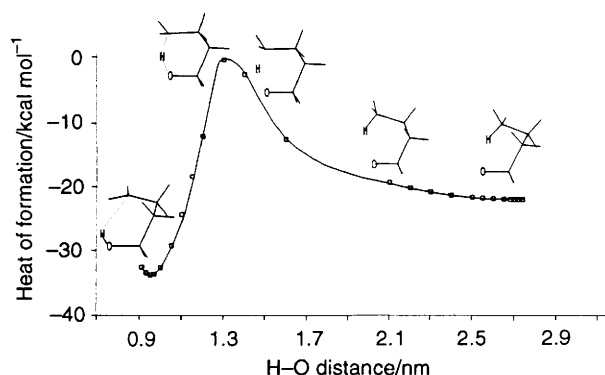


Fig. 3 Energy profile and trajectory of the 1,5-H migration in the butoxy radical, calculated by MNDO-PM3 method

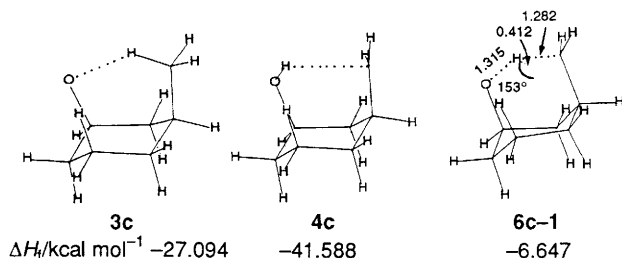


Fig. 4 Structures of radicals **3c**, **4c** and transition state **6c-1**

transition state is stabilised by interaction with σ -orbitals of proper symmetry. Analogous stabilisation of the corresponding transition state in alkoxy radicals is not obvious, because of its lack of symmetry.

The transformation from **3b** to **4b**, i.e. 1,5-H migration, was examined by calculations. The structure of the transition state, **6b-1**, was refined by TS option in MOPAC, and is given in Fig. 2 ($\Delta H_f = -0.076$ kcal mol⁻¹) (Table 1). The migrating hydrogen atom is slightly out of the plane defined by the O-C(α) and C(γ)-C(δ) bonds (ca. 17°); the transition state acquiring a chair-like structure. The vibrational analysis of this structure shows only one negative frequency.

Results of MNDO-PM3 calculations on species derived from the butoxy radical **3b** are in fairly good agreement with *ab initio* results.^{3a} The PM3-MNDO method gives larger differences in heats of formation for the alkoxy and hydroxyalkyl radical (*ab initio* at UMP2/6-31G* level gives almost the same heat of formation for both radicals). The enthalpy of activation for the 1,5-hydrogen migration in the butoxy radical is about 23.2 kcal mol⁻¹ [in ref. 2(a), only 14.9 kcal mol⁻¹ is reported]. Nevertheless, the geometries of the reactant, product, and transition state are very similar to those obtained by *ab initio* calculations.[†]

The lowest energy path for 1,5-H migration and the corresponding diagram of energy change are given in Fig. 3. During the migration of hydrogen from carbon to oxygen, the O-C(δ) distance deviates very little from 0.25 nm (up to 0.257 nm). The geometry of the transition state is very similar to the geometry found by the MM2 method.^{3b}

Before drawing further conclusions about the properties of alkoxy- and hydroxy-alkyl radicals, we performed analogous calculations on radicals derived from *cis*-3-methylcyclohexanol (**1c**). In order to simulate the steroid structure (Fig. 1), the starting geometry of this substrate was considered in a diaxial

[†] It should be noted that *ab initio* geometry of the TS gives larger difference in O-H and C-H bonds, despite the almost equal heats of formation of reactant and product (conflict with the Hammond principle).

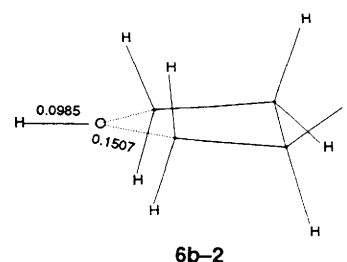


Fig. 5 Transition structure, **6b-2**, for the 1,4-OH migration in 4-hydroxybutyl radical. Distances shown in nm.

conformation. The calculated geometries for radicals **3c**, **4c**, **6c**, together with their heats of formation, are shown in Fig. 4.

The carbon radical **4c** is, as expected, the most stable of the studied species. The energy relationships between radicals **3c** and **6c** are comparable to those of butan-1-ol origin. Radicals **4c** and **3c** are proven to be intermediates, while radical **6c** is the transition state, showing one negative frequency.

The energy partitioning analysis (Table 2) indicates that the differences in radical stabilities arise mainly from the differences in the sums of the bicentric terms. Particularly interesting is the analysis of the mono- and bi-centric contributions related to the OC(δ)H(μ) fragment. The difference in this term in O and C radicals arises mainly from the difference in stabilities of the O-H(μ) and C(δ)-H(μ) bonds in **4c** (**4b**) and **3c** (**3b**), respectively. It is interesting to note that Σ OH(μ) and Σ C(δ)H(μ) terms in **6b(c)** differ considerably [by 1.20 (1.46) eV], indicating that in these radicals H(μ) is more strongly bonded to the carbon than to the oxygen. The Σ O...C(δ) term appears to be slightly repulsive in all of the considered radicals.

This opens the question why cyclisation to **8** is so efficient when O[•] and C(δ)-H in **3** are suitably oriented.

Cyclisation.—In order to get more detailed information about the cyclisation **4**→**8**, we have computationally simulated different modes of the movement of the hydrogen atom away from the rest of the free radical.

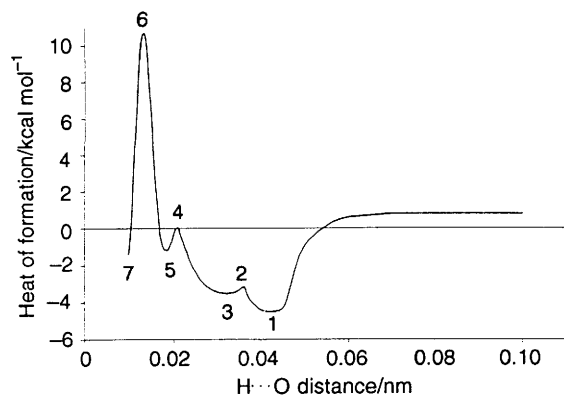
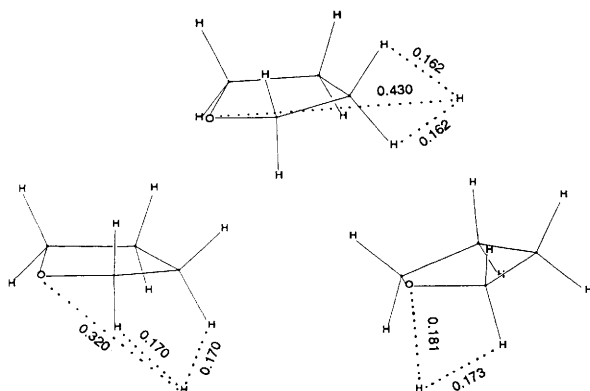
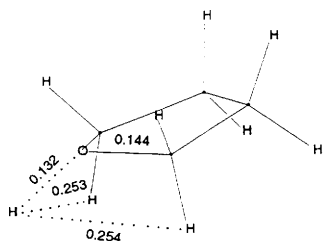
Making the C(δ)...O distance in the C-radical **4b** shorter, the compound passes through a transition state at a distance of ca. 0.15 nm. After this rough estimation, the structure of the transition state was refined using 'TS' option in MOPAC (structure **6b-2**, Fig. 5). At this point the C(α)-O and C(δ)-O bonds have almost identical length. Further reduction of the C(δ)...O distance causes C(α)-O bond scission giving a new hydroxybutyl radical in an extended conformation. This is a reasonable result, because such a product has more bonding interactions than the two separated moieties.

The symmetrical transition state has a heat of formation of only -1.39 kcal mol⁻¹. It is lower than the transition state for hydrogen migration. It means that under given experimental conditions when hydrogen migration occurs, the cyclisation transition state is readily accessible.

The same transition state is obtained by the simulation of the approach of hydrogen atom to oxygen in tetrahydrofuran. The supermolecule with two fragments, H atom and THF, separated 1 nm or more has $\Delta H_f = 0.79$ kcal mol⁻¹. The distance between the hydrogen atom and the ring oxygen was systematically reduced treating it as a reaction coordinate in the frame of MOPAC facilities. The energy profile of this reaction is given in Fig. 6. Along this reaction path several energy minima could be located. First ground state complex (point 1 in Fig. 6) has a H(μ)...O distance 0.41 nm. The stabilising interaction is actually between the ring hydrogens and the approaching H atom (Fig. 7, upper). Heat of formation for this complex is -4.308 kcal mol⁻¹. There are another two ground state complexes between tetrahydrofuran and hydrogen atom,

Table 2 MNDO-PM3 energy partitioning in radicals derived from butan-1-ol (**1b**), and *cis*-3-methylcyclohexanol (**1c**) (eV)^a

	$\Sigma M\cdot +$	$\Sigma B\cdot +$	$\Sigma_{\text{M}}\text{OC}(\delta)\text{H}$	$\Sigma \text{O}\cdots\text{C}(\delta)$	$\Sigma \text{O}\cdots\text{H}$	$\Sigma \text{C}(\delta)\text{H}$	$\Sigma_{\text{B}}\text{OC}(\delta)\text{H}$
3b	-738.72	-164.07	-385.25	0.460	-0.10	-12.68	-12.31
4b	-737.36	-166.09	-384.12	0.322	-13.17	-0.362	-13.93
6b	-738.74	-163.67	-385.05	0.487	-5.99	-7.19	-12.69
3c	-1057.26	-263.03	-385.30	0.097	-0.12	-12.63	-12.65
4c	-1055.78	-265.27	-384.15	0.322	-13.83	-0.37	-13.88
6c	-1057.24	-262.72	-385.13	0.479	-5.82	-7.28	-12.62

^a The hydrogen atom involved, is the one subjected to the migration (expulsion).**Fig. 6** Potential energy curve for the approach of hydrogen atom to the oxygen atom in tetrahydrofuran. Point '7' corresponds to the structure in Fig. 5.**Fig. 7** Structure of complexes that corresponds to the points '1' (top), '3' (bottom left) and '5' (bottom right) in Fig. 6. Distances shown in nm.**Fig. 8** Structure of the transition state for the approach of the hydrogen atom toward the ring oxygen of tetrahydrofuran (**6b-3**), corresponding to the maximum in Fig. 6. Distances shown in nm.

having $\text{O}\cdots\text{H}$ distances 0.320 and 0.183 nm, respectively (Fig. 7, bottom). Still, there is almost no perturbation on the tetrahydrofuran ring.

Several transition states can be located along the reaction path of the $\text{O}-\text{H}$ bond formation. In the highest one (that corresponds to point 6 in Fig. 6) the tetrahydrofuran ring is not considerably distorted. Both $\text{C}-\text{O}$ bonds are almost of the same

length as in tetrahydrofuran (0.144 nm). The approaching hydrogen atom is 0.133 nm away from oxygen (Fig. 8). The vibrational analysis of this transition state gives only one negative frequency. The energy of the transition state amounts to 10.692 kcal mol⁻¹, and is considerably higher than that for 1,5-H migration. Further decrease in $\text{O}\cdots\text{H}$ distance leads to another stationary point on the potential energy hypersurface (point 7, Fig. 6). It is another transition state, exactly the same one shown on Fig. 5. It was not possible to locate the minimum between these two transition states, because the second one is actually very flat (negative vibration is only -218 cm⁻¹), and all searches end in 4-hydroxyalkyl radical **4b**. The reversal of the just described reaction path illustrates the cyclisation to tetrahydrofuran. The overall activation barrier for hydrogen abstraction from the hydroxyalkyl radical is very high (44.10 kcal mol⁻¹, or 32.54 kcal mol⁻¹ starting from alkoxy radical).

The most probable mode for the hydrogen atom separation is its abstraction from the $\text{C}(\delta)$ atom in radical **3** promoted by the interaction with oxygen. Applying the Marcus theory⁶ on the data about ground and transition state energies for hydrogen abstraction and migration, it is estimated that there is no considerable activation barrier for the transfer between the two transition states, **6b-1** and **6b-2**.

The hydrogen abstraction from oxygen in radical **4b** cannot be ruled out. The perfect match of transition state **6b-2**, obtained by variation of the $\text{O}-\text{C}(\delta)$ distance, into the PE curve for approach of the H-atom to oxygen of tetrahydrofuran (Fig. 6), indicates that approach of O and $\text{C}(\delta)$ atoms can be followed (or accompanied) by hydrogen removal.

For the cyclisation of the butoxy radical **3b** two reaction paths can be postulated. (a) Starting from the C-radical: **4b**→**6b-1**→**6b-2**→**8b**, the energy barrier is 44.10 kcal mol⁻¹. (b) Starting from the O-radical: **3b**→**6b-1**→**6b-2**→**8b**, the activation barrier is somewhat lower: 33.92 kcal mol⁻¹. Anyway, it is not likely that this hydrogen abstraction will spontaneously take place. But, if a hydrogen acceptor is present, e.g. another radical species, the activation energy should be much lower (according to Marcus' theory and Hammond's principle, the potential energy barrier can be reduced by lowering the energy of the final state).

To estimate the reliability of the results obtained, as a reference *ab initio* values for the ethoxy and hydroxyethyl radicals can be used.⁵ (The corresponding activation barriers are 48.06 kcal mol⁻¹ and 33.30 kcal mol⁻¹ for hydrogen abstraction from the ethoxy and the hydroxyethyl radical, respectively.) Due to the larger substitution, activation energies in the butoxy radical should be somewhat lower.

All the characteristic structures identified for the cyclisation process of the butoxy radical (structures of the O and C radicals and of the various transition states are given in Figs. 5-8) have their analogues in the cyclisation of the *cis*-3-hydroxycyclohexylmethyl radical. The transition state for 1,4-migration of the OH group is shown in Fig. 9, left. The energy of this transition state, **6c-2**, is slightly higher than the TS for hydrogen migration (Fig. 4). The next transition state for hydrogen

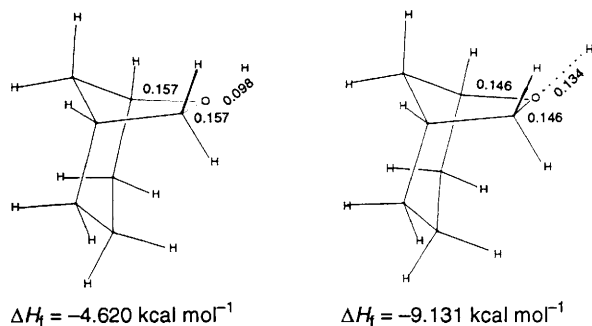


Fig. 9 Structures of the transition states for 1,4-OH migration, **6c-2** (left), and hydrogen abstraction, **6c-3** (right), in *cis*-3-hydroxycyclohexylmethyl radical. Distances shown in nm.

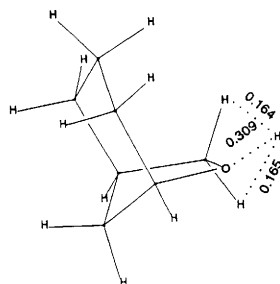


Fig. 10 Complex of ether **8c** with hydrogen atom. Distances shown in nm.

abstraction, **6c-3**, is given in Fig. 9, right. Both structures are proven to be transition states by their vibration analysis, showing only one vibration frequency. The energy difference between these two transition states is almost the same as in the case of the butoxy radical. Structural details given in Fig. 9 can be compared with those in Figs. 5 and 8. The complex between the resulting cyclic ether and hydrogen atom shown in Fig. 10 has similar features as those in Fig. 7.

The close analogy of structural features of intermediates and transition states derived from butoxy- and *cis*-3-methylcyclohexyloxy radicals enables the extension of the discussion given for cyclisation to tetrahydrofuran, to its higher homologue.

Conclusions

From our calculations the following conclusions can be drawn. (a) Radical **4** is more stable than radical **3**. Hydrogen migration from the δ -carbon to oxygen takes place with rather low activation energy, when C(δ) and O are conveniently spatially oriented. (b) During migration, the hydrogen atom is mostly in

the plane corresponding to the chair conformation of a six membered cyclic transition state. (c) Due to a high activation energy, hydrogen abstraction will be accomplished only with the assistance of a hydrogen atom acceptor. It is most probable that it should take place before the formation of radical **4**. (d) The transition state for hydrogen abstraction is very similar to the cyclic ether product, *i.e.*, cyclisation takes place prior to expulsion of the hydrogen atom. This perfectly matches the experimental finding that efficiency of cyclisation strongly depends on the stereochemistry of the substrate. (e) The transition state energy for ring closure in hydroxyalkyl radicals is lower than, or of very similar energy as, that for hydrogen migration. The observed 'memory effect' is a normal consequence when ring closure takes place before, or concurrently to the completion of hydrogen migration to oxygen. In the case of sterically rigid alcohols, the geometry of radical **3** allows relatively easy migration and/or cyclisation, and, therefore, the formation of the carbonium-ion **5** is not very probable. In the case of flexible alcohols, the corresponding transformation is confronted with a relatively high conformational barrier, and transformation **3**→**6**→**8** must compete with other transformation paths (**3**→**9**, **3**→**4**→**10**, **3**→**4**→**5**→**11**).

References

- (a) M. Lj. Mihailović and Ž. Čeković, *Synthesis*, 1970, 209; (b) R. H. Hesse, *Advances in Free-radical Chemistry*, 1969, 3, 83; (c) K. Heusler and J. Kalvoda, *Angew. Chem.*, 1964, **76**, 518, *Angew. Chem., Int. Ed. Engl.*, 1964, **3**, 525; (d) M. Lj. Mihailović and R. E. Partch, in *Selective Organic Transformations*, ed. B. S. Thyagarayan, Wiley-Interscience, New York, London, 1972, vol. 2, pp. 97-182.
- (a) R. C. Bingham, M. J. S. Dewar and D. H. Lo, *J. Am. Chem. Soc.*, 1975, **97**, 1285; (b) P. Bischof, *Croat. Chem. Acta*, 1980, **53**, 51; (c) M. J. S. Dewar, G. Ford, H. S. Rzepa and Y. Yamaguchi, *J. Mol. Struct.*, 1978, **43**, 1325; (d) J. J. P. Stewart, *QCPE*, No. 455; (e) H. S. Rzepa and W. A. Wylie, *J. Chem. Soc., Perkin Trans. 2*, 1991, 939.
- (a) A. E. Dorigo, A. McCarrick, R. J. Loncarich and K. N. Houk, *J. Am. Chem. Soc.*, 1990, **112**, 7508; (b) A. E. Dorigo and K. N. Houk, *J. Org. Chem.*, 1988, **53**, 1650.
- J. W. Verhoeven and P. Pasman, *Tetrahedron*, 1981, **37**, 943.
- C. Sosa and H. B. Schlegel, *J. Am. Chem. Soc.*, 1987, **109**, 7007.
- (a) R. A. Marcus, *J. Phys. Chem.*, 1968, **72**, 891; (b) S. Wolfe, D. J. Mitchell and H. B. Schlegel, *J. Am. Chem. Soc.*, 1981, **103**, 7692 and 7694.
- A. R. Srinivasan and W. K. Olson, *J. Chem. Educ.*, 1989, **66**, 664; E. Hamori, R. D. Broad and C. E. Reed, Jr., *Perception*, 1992, **11**, 297. Right-hand pair of stereo-drawings enables the unaided cross-eyed stereopsis.

Paper 3/06001B

Received 7th October 1993

Accepted 8th December 1993